

Field-dependent magnetization for an Anderson model fluctuating between two magnetic configurations

This article has been downloaded from IOPscience. Please scroll down to see the full text article.

1993 J. Phys.: Condens. Matter 5 L541

(<http://iopscience.iop.org/0953-8984/5/44/001>)

[View the table of contents for this issue](#), or go to the [journal homepage](#) for more

Download details:

IP Address: 171.66.16.96

The article was downloaded on 11/05/2010 at 02:08

Please note that [terms and conditions apply](#).

LETTER TO THE EDITOR

Field-dependent magnetization for an Anderson model fluctuating between two magnetic configurations

J M Landgraf and J W Rasul

The Harrison M Randall Laboratory of Physics, University of Michigan, Ann Arbor, MI 48109-1120, USA

Received 23 August 1993

Abstract. We calculate the magnetization as a function of field for an Anderson impurity model for which the lowest configurations are f^1 and f^2 , using the leading order $1/N$ expansion (where N is the orbital degeneracy). For most values of the valence, except those near two, we find a two-stage crossover in $M(H)$. This is due to an unbinding of the many-body singlet, first to a partially screened magnetic state and then to the full f^2 moment. At small fields there is a positive deviation from linearity in $M(H)$ near the integer valent limits which is characteristic of degenerate f^0-f^1 models. This upturn disappears for intermediate values of the valence.

The problem of a magnetic impurity embedded in a metal has occupied the attention of experimental and theoretical physicists for several decades [1]. In recent years the problem has attracted most attention in the context of dilute rare-earth and actinide systems, particularly those that show heavy-electron behaviour [2]. Whilst the cerium impurity model has attracted most attention and has seen considerable progress, the problem of dilute rare-earth and actinide systems where both of the two lowest atomic configurations are degenerate has, until recently, received comparatively little attention.

The recent interest in this problem has focussed on the ‘non-Fermi liquid’ behaviour expected when impurity states couple to electronic states of different degeneracy, such as when the local moment has quadrupolar character [3] or when additional long-range interactions [4] are included. Apart from the well known example of high- T_c systems in their normal state, non-Fermi liquid behaviour is also seen, for example, in $U_{1-x}Pd_3Y_x$ [5]. For these model systems, exact numerical renormalization group (RG) and mappings onto Bethe *ansatz* soluble models confirm the overcompensated non-Fermi liquid of the ground state. Similarly for undercompensated models, such as when the number of electronic channels is insufficient to screen the impurity, RG and Bethe *ansatz* results are also available [6].

The case where the f^1 and f^2 states couple to electronic states of the same symmetry [7–14] has been studied in a number of works. Few exact results exist, except for a recently reported numerical renormalization group treatment on a ($j = 2$) f^1 state mixing with a ($j = 3/2$) f^2 state [13]. The ground state for such a model is a many-body singlet, in agreement with the results of earlier variational [7, 9, 10], $1/N$ expansion [8, 10, 14], and NCA [11] approaches. For the f^1-f^2 model with $j-j$ coupling the present authors recently calculated the valence photoemission spectra [14] and found the persistence of a Kondo-like peak for all valences which contained a substantial fraction of the total weight in the intermediate valence regime. The upshot of all these studies is that a small Kondo-like energy scale characterizes the formation of the many-body singlet even when the valence fluctuations are strongest. Less explored is the stability of this many-body singlet under

changes in temperature and field. The numerical RG study [13] showed that the susceptibility as a function of temperature crosses over from Pauli-like behaviour at low temperature to full local moment behaviour at high temperature, for values of the valence close to two. For intermediate valence, however, a two-stage crossover to the full f^2 moment was obtained, which was interpreted as a partial unbinding of the many-body singlet. For valences close to one, the two-stage effect again took place, but over a much larger temperature region.

In magnetic impurity problems a correspondence holds between magnetic field and temperature—both are effective in driving the system through the crossover region. One would then naturally expect the features found in the temperature dependence in the RG calculation [13] to be repeated in the zero-temperature field-dependent magnetization. Although from an experimental point of view one expects only the small-field region to be accessible, one knows from experience with the f^0-f^1 problem that, even for the small-field region, qualitatively different behaviour is seen depending on the impurity degeneracy. For spins less than $j = 3/2$ the exact solution of the Coqblin-Schrieffer model shows a downward curvature in the magnetic isotherms whereas for spins equal to or greater than $3/2$ the curvature is positive [15]. Such an upward curvature, for $j = 7/2$, fits the experimental measurements on YbCuAl [16]. For this reason a knowledge of the field-dependent magnetization of the f^1-f^2 model would be of considerable importance.

For the f^1-f^2 problem where no exact solution is available the only readily implementable treatment (short of an RG one) is with the aid of the $1/N$ or variational ground-state method [7, 8, 9, 10] which can be straightforwardly extended to finite field in order to investigate the questions mentioned above. From experience with the f^0-f^1 problem it is known that the finite-field large- N problem exhibits some unphysical features [17]: slave-boson methods obtain a second-order phase transition in the auxiliary boson field, which in the magnetization is reflected in a discontinuity of slope at the crossover field. Subtle generalizations of the Zeeman splitting scheme have to be invoked if one is to avoid this transition [18]. However, the large- N limit for the f^0-f^1 model does obtain the qualitative features at low field correctly, namely an upturn in the magnetic isotherm [17], while above the critical crossover field the magnetization takes on its full moment value.

For the above reason we shall use the large- N variational wavefunction for the f^1-f^2 problem at large but finite N . This has the effect of smoothing out the singlet magnetic state crossover while at the same time determining the overall physics of the crossover correctly. We will show that the crossover to magnetic behaviour can be correctly described with the same variational wavefunction that yields a singlet at low fields. While the large- N calculation is no substitute for an exact calculation, we do, on the basis of experience with the f^0-f^1 problem, expect the qualitative features mentioned earlier to be reproduced. We shall be particularly interested in how these features, namely, the nature of the crossover and the low-field behaviour, depend on the impurity valence.

We examine an N -fold degenerate f^1-f^2 Anderson model to leading order in the $1/N$ expansion. For our purposes, f^0 and f^3 character states are assumed to have very high energies and are projected out. Both the Pauli paramagnetism of the conduction band and the contribution of the magnetic impurities will determine the magnetization of such a system. As we are interested in the magnetic effects of the impurities, we take the conduction electron g -factor to be zero. The starting point then is the Hamiltonian:

$$\mathcal{H} = \sum_{k,\mu} \epsilon_k c_{k\mu}^\dagger c_{k\mu} + V \sum_{k,\mu} \{ f_\mu^\dagger c_{k\mu} + c_{k\mu}^\dagger f_\mu \} + \sum_{\mu} (E_1 - g\mu_B H \mu) |\mu\rangle\langle\mu| + \sum_{\mu<\mu'} (E_2 - g\mu_B H(\mu + \mu')) |\mu, \mu'\rangle\langle\mu, \mu'| \quad (1)$$

where $c_{k\mu}^\dagger$ represent creation operators for electron states with momentum k and angular momentum μ , f_μ^\dagger represent local state operators with angular momentum μ , and E_1 and E_2 represent the zero-field bare atomic state energies for one and two f electrons respectively, g is the f electron g-factor, μ_B is the Bohr magneton, and H is the applied field. The hybridization matrix element V is taken to be momentum independent and we assume a flat density of states ρ cut off at bandwidth $\pm D$. The hybridization between local and band states only occurs for states of the same symmetry with hybridization width $\Gamma = \rho_0 V^2 N$.

To leading order in $1/N$ each f electron is screened by a hole in the conduction band with the same angular momentum, and particle-hole pair states are ignored. In the restricted basis that results, the ground-state wavefunction may be written

$$|\Psi_0\rangle = \sum_{\epsilon, \mu} \alpha_\mu(\epsilon) c_{\epsilon\mu} f_{\epsilon\mu}^\dagger |0\rangle + \sum_{\substack{\epsilon, \epsilon' \\ \mu < \mu'}} \beta_{\mu\mu'}(\epsilon, \epsilon') c_{\epsilon\mu} f_\mu^\dagger c_{\epsilon'\mu'} f_{\mu'}^\dagger |0\rangle \quad (2)$$

where the ϵ summations are cut off at the Fermi energy. Despite the fact that this ground state is necessarily an angular momentum singlet, it may carry a magnetic moment because only the f-electron states couple to the magnetic field. The amplitudes $\alpha_\mu(\epsilon)$ and $\beta_{\mu\mu'}(\epsilon, \epsilon')$ are then obtained by applying the time-independent Schrödinger equation $\mathcal{H}|\Psi\rangle = E_0|\Psi\rangle$. This leads, after some algebra, to the following integral equations for $\alpha_\mu(\epsilon)$ and $\beta_{\mu\mu'}(\epsilon, \epsilon')$:

$$(E_{10} - \epsilon - g\mu_B\mu H)\alpha_\mu(\epsilon) = V^2 \sum_{\substack{\epsilon', \mu' \\ \mu' \neq \mu}} \frac{\alpha_\mu(\epsilon) + \alpha_{\mu'}(\epsilon')}{E_{20} - \epsilon - \epsilon' - g\mu_B(\mu + \mu')H} \quad (3)$$

$$\beta_{\mu\mu'}(\epsilon, \epsilon') = V \frac{\alpha_\mu(\epsilon) + \alpha_{\mu'}(\epsilon')}{E_{20} - \epsilon - \epsilon' - g\mu_B(\mu + \mu')H}. \quad (4)$$

Here, the separation $E_{21} = E_2 - E_1$ is taken as a model parameter and the ground-state energy E_{20} is determined by the first of these equations.

The integral equations (3) and (4) are in fact a set of N coupled integral equations. They may be solved by observing that if we solve the single-integral equation

$$D(-x)\tilde{\alpha}(x) = V^2 \rho \int_{-D-\Delta}^0 dx \sum_{\mu'=-J}^J \frac{\tilde{\alpha}(x')}{\epsilon_{20} - x - x'} \quad (5)$$

where

$$D(-x) = E_{10} - x - V^2 \rho \int_{-D}^0 d\epsilon \sum_{\mu'=-J}^J \frac{1}{(E_{20} + g\mu_B H \mu' - \epsilon - x)}$$

then by using the substitution

$$\alpha_\mu(\epsilon) = \tilde{\alpha}(\epsilon - g\mu_B H \mu) \quad (6)$$

we note that equation (3) is satisfied apart from corrections of order Γ/N , which represent the effect of the Pauli exclusion principle in the f^2 state.

Typically when working within the $1/N$ expansion at leading order, one takes an infinite f-level degeneracy and considers the results of the theory to be exact for this unphysical model. Presently, however, it is more convenient to hold N finite, and treat the leading order in $1/N$ as an approximation to the exact result. It is possible to write this theory for $N \rightarrow \infty$ by taking $g \rightarrow 0$ such that $\Delta = g\mu_B H N$ remains finite. Then we may write

equation (3) in terms of integrations over spin indices. Unfortunately, such a treatment fails for even moderate fields because the change of variables (6) leads to a Jacobian which has zero weight at $x = 0$, while the wavefunction $\tilde{\alpha}^\infty(x)$ has nearly all of its weight in the lowest-energy spin channel and hence near $x = 0$. In order to correctly handle this effect, one would have to handle the lowest-energy channel separately—in which case the substitution (6) would no longer be valid. We consider, instead, the case of finite f-electron degeneracy.

We solve equation (5) using a method by which we guess a solution and iteratively improve the guess until we obtain consistent results for E_{20} and $\tilde{\alpha}(\epsilon)$ [8, 9]. The magnetization is obtained by directly calculating the occupancy of each atomic channel:

$$M = \int_{-D}^0 d\epsilon \sum_{\mu=-J}^J \mu g \mu_B (\alpha_\mu(\epsilon))^2 + \int_{-D}^0 d\epsilon \int_{-D}^0 d\epsilon' \sum_{\mu'=-J}^J \sum_{\mu=-J}^J (\mu + \mu') g \mu_B (\beta_{\mu\mu'}(\epsilon, \epsilon'))^2. \quad (7)$$

Alternatively it may be noted that the above expression is nothing other than

$$M = \langle \Psi_0 | -\partial \mathcal{H} / \partial H | \Psi_0 \rangle = -\partial E_0 / \partial H = \partial E_{20} / \partial H. \quad (8)$$

It is also possible to calculate the energies of states for which the atomic moments are unscreened or only partially screened. For the case of unscreened states (analogous to the ‘no-hole triplet’ of [9]) the wavefunction is,

$$|\Psi_{\mu,\mu'}\rangle = f_\mu^\dagger f_{\mu'}^\dagger |0\rangle \quad (9)$$

which has an energy $E_{\mu,\mu'} = E_2 - g \mu_B H(\mu + \mu')$.

For the case of partially screened states (analogous to the ‘doublets’ of [7, 9, 10]) the derivation of the wavefunction proceeds analogously to that of the ground state. The wavefunction for the partially screened state is written

$$|\Psi_m\rangle = \alpha f_\mu^\dagger |0\rangle + \sum_{\epsilon,\mu'} \beta_{\mu'}(\epsilon) c_{\epsilon\mu'} f_{\mu'}^\dagger f_\mu^\dagger |0\rangle \quad (10)$$

which leads to transcendental equations for the magnetic state energies:

$$D^m(0) = E_{10}^m + g \mu_B H \mu - V^2 \rho \int_{-D}^0 d\epsilon' \sum_{\mu'=-J}^J \frac{1}{(E_{20}^m - \epsilon' - g \mu_B H(\mu + \mu'))} = 0 \quad (11)$$

where E_{10}^m (E_{20}^m) is the separation of the partially screened magnetic state energy and the bare f^1 (f^2) state. These magnetic states are significant for two reasons. When no magnetic field is applied, the energy separation between the magnetic and ground state represents a spin fluctuation energy scale which controls the magnitude of the magnetic susceptibility. Secondly, as the magnetic field is applied the energy separation between the ground state (2) and magnetic state (11) becomes very small. Therefore, by equation (8), the magnetization of the ground state closely follows that of the magnetic state.

This second result may be understood by considering equation (3) for large magnetic fields compared with the singlet-magnetic separation at zero field. In this case, only the occupation of the lowest-energy spin channel is significant and the sum on the right-hand side is restricted to a single term. The equation is then identical to that of the magnetic state, apart from a Γ/N correction, so that the singlet-magnetic separation remains extremely small. This point emerges quite clearly in the numerical solutions, as we shall see later.

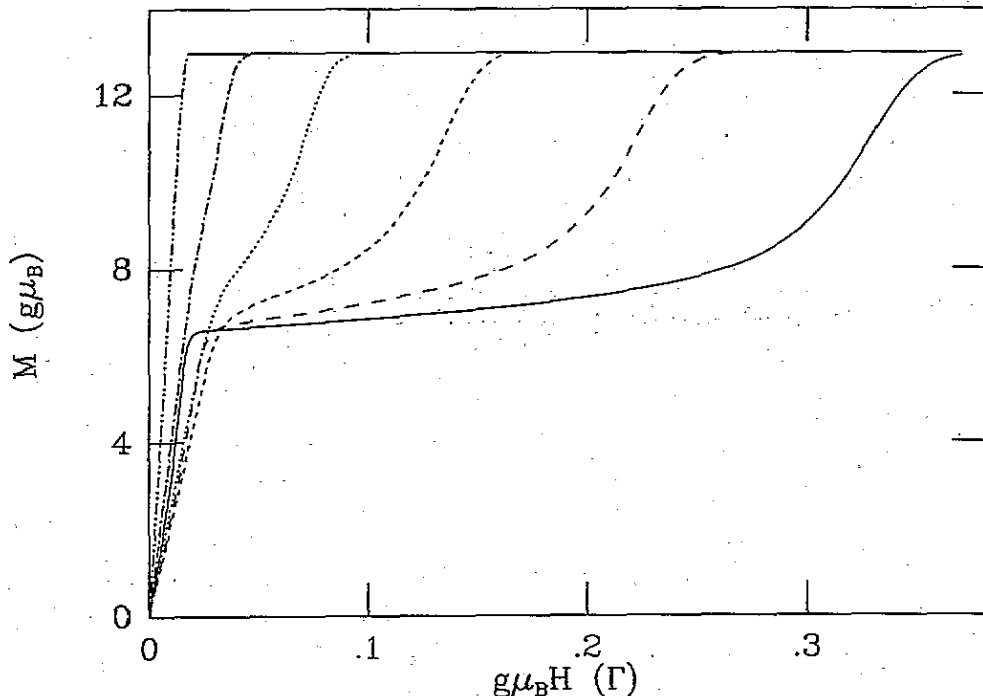


Figure 1. The magnetization as a function of applied field in units of the hybridization width for $E_{21} = 0$ (solid line), $E_{21} = -1$ (long dashes), $E_{21} = -2$ (short dashes), $E_{21} = -3$ (dots), $E_{21} = -4$ (dash-dot), $E_{21} = -5$ (dash-dot-dot). Here the bandwidth, D , is 10Γ , and the orbital degeneracy, N , is 14.

Turning to the numerical results for the magnetization (7) we show in figure 1 the full magnetic-field dependence (on a scale given by the hybridization width Γ) of this quantity, for a set of values of the bare atomic splitting E_{21} with a value of the bandwidth equal to 10Γ and an f-level degeneracy of 14. In all cases we see the initial linear dependence eventually saturate. In the region where the valence is close to two ($n_f = 1.91$ for $E_{21} = -5$ and $n_f = 1.83$ for $E_{21} = -4$) there is a single crossover to a saturated value equal to the full f^2 moment (in this case $13g\mu_B$). As the valence moves to smaller values ($n_f = 1.71$ for $E_{21} = -3$) a shoulder begins to appear in the crossover region which turns into a distinct plateau as the valence moves towards the f^1 region. For the lowest value shown ($n_f = 1.34$ for $E_{21} = 0$) this plateau region holds for a considerable field region roughly proportional to the energy separation between the bare f^2 state and the magnetic state (11) (or, just as accurately in this region, the ground state (2)).

In figure 2 we show the valence as a function of applied field. In all cases the valence tends towards two for large magnetic fields. In the region of small zero-field valence there is a small, but sharp reduction in valence at a field a few times the singlet-magnetic separation δ .

One may consider the role of hybridization in this model in two steps. First the hybridization between the f^1 and f^2 states leads to an energy reduction of the partially screened magnetic states as compared to their bare atomic energies. Secondly, the hybridization between various spin channels (of the f^1 states) further reduces the energy of the singlet beyond that of the partially screened magnetics states. The energy scale

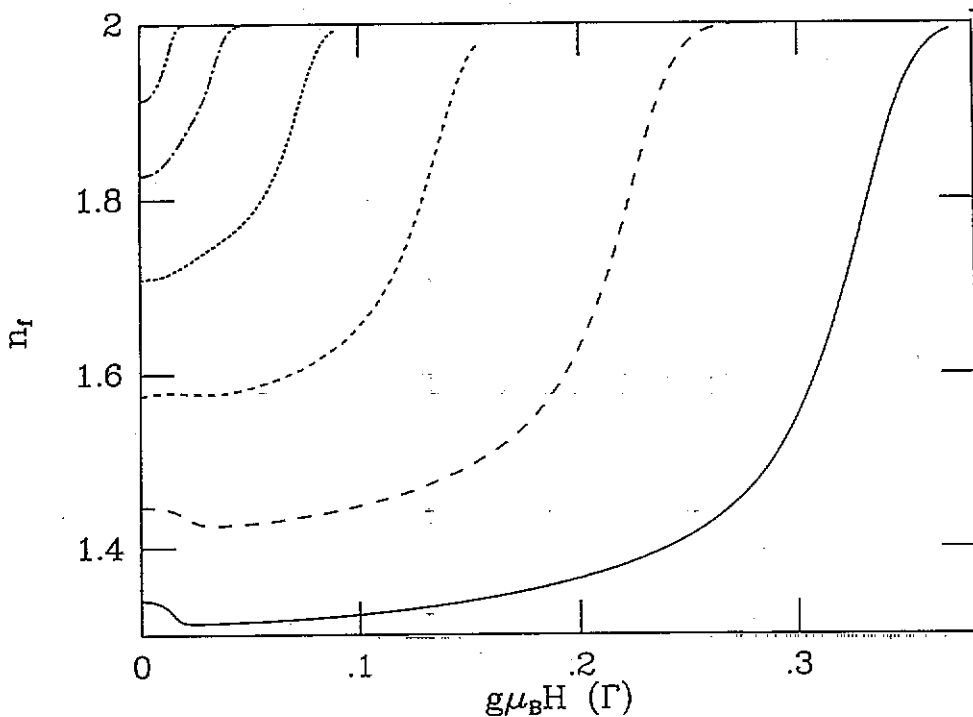


Figure 2. The valence as a function of applied field in units of the hybridization width for $E_{21} = 0$ (solid line), $E_{21} = -1$ (long dashes), $E_{21} = -2$ (short dashes), $E_{21} = -3$ (dots), $E_{21} = -4$ (dash-dot), $E_{21} = -5$ (dash-dot-dot). Here the bandwidth is 10Γ and the orbital degeneracy is 14.

associated with the first process is E_{20}^m and that of the second process is δ , the singlet-magnetic separation.

This leads to a simple description of the two-stage effect of the magnetization with field—as well as the behaviour of the valence. When the field is applied it lowers the energy of certain magnetic states. When the field is large enough so that this energy, $g\mu_B H_j \approx g\mu_B HN/2$, is greater than δ , the ground state will become polarized, so that only the lowest magnetic channels are substantially occupied. In this case there will be very little overlap between different f^1 channels and the energy of the ground state will be very near that of the partially screened magnetic states. So far we have neglected the ability of the singlet state to minimize its energy by a combination of hybridization and polarization. From our numerical results we see that this leads to a slightly higher crossover field $g\mu_B NH \approx 4\delta$. Even though the ground state is still an angular momentum singlet, the magnetization ($M = \partial E_{20} / \partial H$) and valence ($n_f = \partial E_{20} / \partial E_{21}$) follow that of the partially screened magnetic state, and we may consider the singlet state ‘unbound’. We can see this very clearly for the magnetization in figure 3 where, after the field reaches $g\mu_B H \approx 4\delta/N$, the magnetization of the polarized singlet state is very near that of the magnetization of the partially screened magnetic states. This also accounts for the sharp valence reduction of the singlet state with magnetic field for the $E_{21} = 0$ and $E_{21} = -1$ curves because the valence, in absence of field, of the partially screened magnetic states is slightly smaller than that of the singlet state.

In the same manner, when the energy gained by the completely unscreened f^2 states as

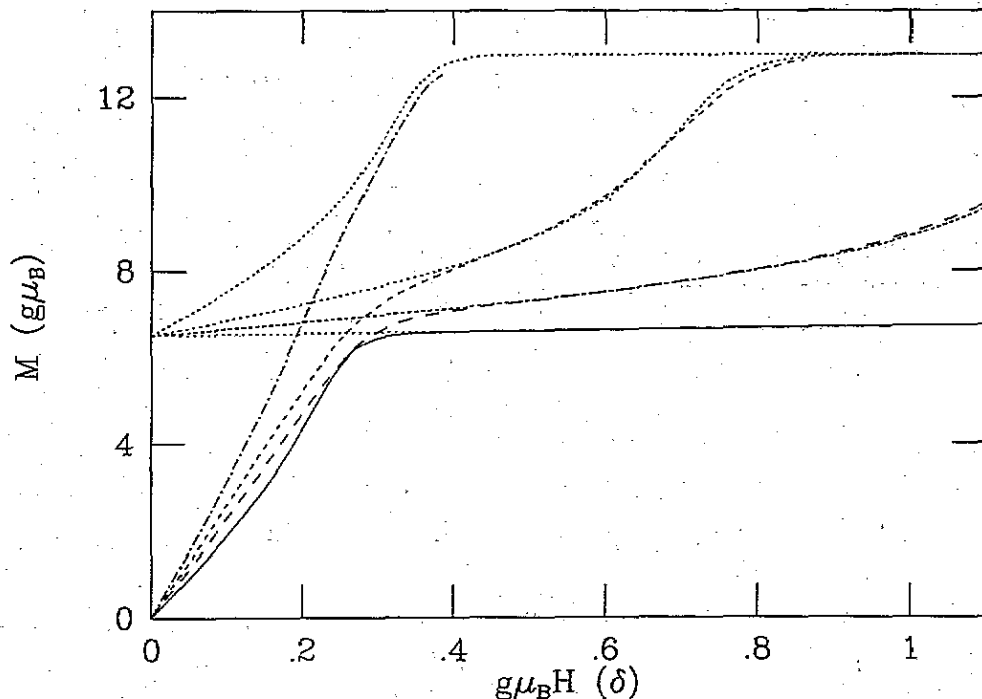


Figure 3. The magnetization as a function of applied field in units of δ , the zero-field singlet-magnetic separation for $E_{21} = 0$, $\delta = 0.064\Gamma$ (solid line), $E_{21} = -2$, $\delta = 0.108\Gamma$ (long dashes), $E_{21} = -3$, $\delta = 0.103\Gamma$ (short dashes), $E_{21} = -5$, $\delta = 0.042\Gamma$ (dash-dot). Also plotted is the magnetization of the partially screened magnetic states (dots) for the same parameters. Note that the magnetization of the ground state follows that of the magnetic states very closely for fields greater than $g\mu_B H \approx 4\delta/N$. The bandwidth is 10Γ , and the orbital degeneracy is 14.

compared to that of the partially screened states is comparable to the energy saved by the hybridization between the f^1 and f^2 states E_{20}^m , then the amplitude of the ground state in the f^1 part of the wavefunction will be negligible. Then the overlap between the f^1 and f^2 states is negligible and the energy, and hence magnetization and valence, will cross over to that of the totally unscreened magnetic states ($M = 13$, $n_f = 2$ in the present case). This occurs at fields $g\mu_B H = 2E_{20}$.

Thus, we have demonstrated an almost complete qualitative correspondence between the behaviour of $\chi(T)$ in the renormalization group calculation [13] with $M(H)$ in the present calculation. The physics of the problem is then most readily understood as a two-stage unbinding of the Kondo-like bound state. For valences close to two the separation is hardly visible because the energy scales δ and E_{20}^M are the same in this case (though the $E_{21} = -4$ curve in figure 1 could be said to show a slight feature). The present calculation, together with [13], and that of [10], where the dynamic susceptibility is found to have a two-peak structure, shows that the physics of the f^1-f^{1+1} Anderson model is richer in structure than would be expected on the basis of the results of the f^0-f^1 model.

Experimentally, the most interesting region is the small-field part of the magnetic isotherm. In figure 4 this is shown for the above set of bare atomic splittings as a function of field (in units of δ , the singlet-magnetic splitting in the absence of a field). Plotting the curves in this way shows how the product of the susceptibility with the singlet-magnetic

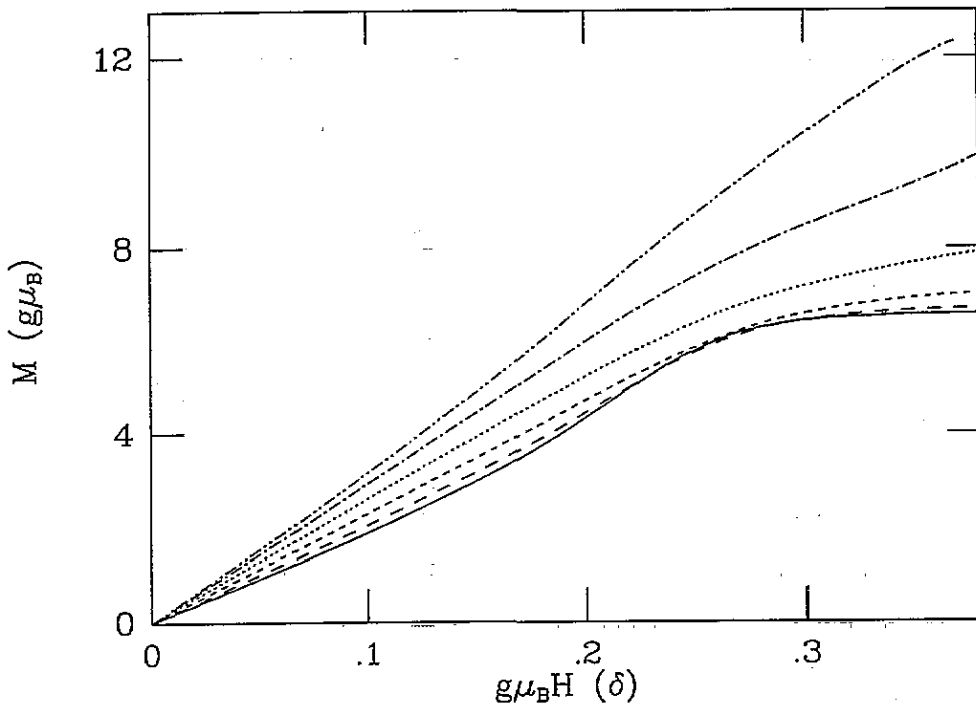


Figure 4. The magnetization for small fields as a function of the applied field in units of δ , the zero-field singlet-magnetic separation, for $E_{21} = 0$, $\delta = 0.064\Gamma$ (solid line), $E_{21} = -1$, $\delta = 0.091\Gamma$ (long dashes), $E_{21} = -2$, $\delta = 0.108\Gamma$ (short dashes), $E_{21} = -3$, $\delta = 0.103\Gamma$ (dots), $E_{21} = -4$, $\delta = 0.075\Gamma$ (dash-dot), $E_{21} = -5$, $\delta = 0.042\Gamma$ (dash-dot-dot). Here the bandwidth is 10Γ and the orbital degeneracy is 14.

splitting increases monotonically with valence. More important, however, is the behaviour of the curves beyond the linear region. A distinct upward curvature exists for values of the valence close to the integer valent limits. This is consistent with expectations based on experience with the integer valence limits of the Coqblin-Schrieffer model, both from exact [16] and large- N [15] treatments. However the upward curvature is no longer evident for values of the valence in the middle of the valence regime. In figure 5 we show a more careful analysis of the departure of M from χH as a function of H/δ . Clearly the upward curvature disappears in the middle of the valence regime.

The implications for actinide impurity systems are that they will not show the upturn found in degenerate Kondo systems such as YbCuAl [15, 16]. Since large- N treatments are known to exaggerate the extent of the upturn in $M(H)$ for the f^0-f^1 model, as compared with exact finite- N results [17], we may expect that for practical values of the degeneracy in the valence fluctuation regime, $M(H)$ might show downward curvature. It is certainly the case for the light heavy-fermion compound UAl_2 [19] that the magnetization is almost linear in H up to 40 T and shows a slight downturn at the lowest temperatures. Moreover, we may expect, on the basis of the close analogy between field and temperature that a downward curvature in $M(H)$ will be accompanied by a negative T^3 term in the specific heat, $C(T)$, at low temperatures (as in the Coqblin-Schrieffer model [1]). The negative T^3 term in $C(T)$ has been recognized for actinide heavy-fermion systems for some time, notably in UBe_{13} [20], UIr_3B_2 [21], and has been regarded [22] as an indication of the

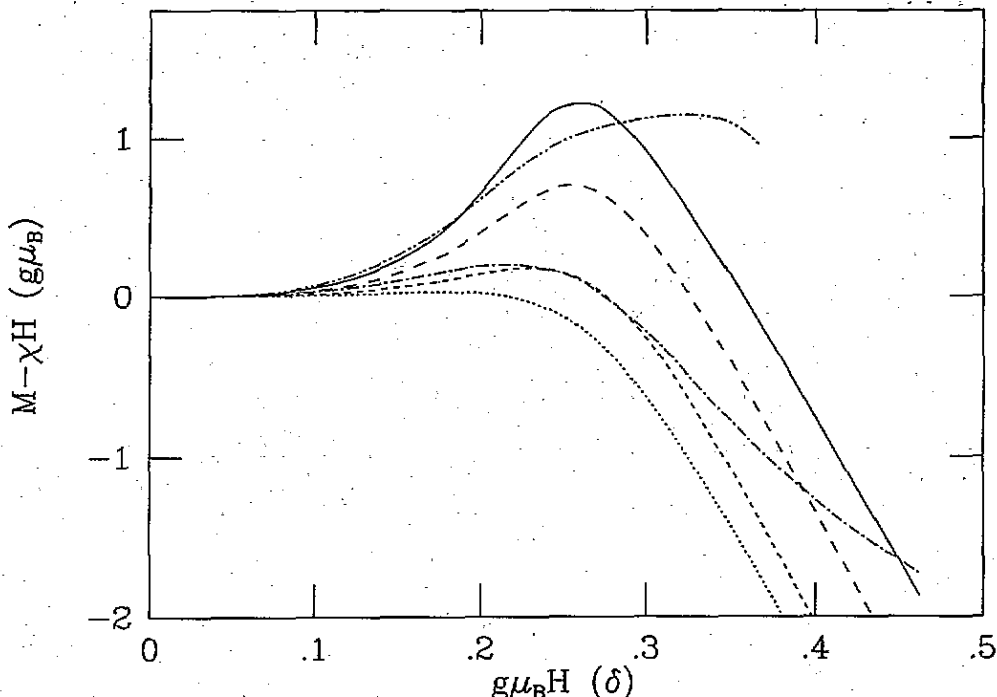


Figure 5. The deviation from linearity of the magnetization as a function of applied field in units of δ , the zero-field singlet-magnetic separation, for $E_{21} = 0$ (solid line), $E_{21} = -1$ (long dashes), $E_{21} = -2$ (short dashes), $E_{21} = -3$ (dots), $E_{21} = -4$ (dash-dot), $E_{21} = -5$ (dash-dot-dot). Note that in the integer valence limits there is a positive deviation for small fields which disappears in the intermediate valence region. Here the bandwidth is 10Γ , and the orbital degeneracy is 14.

inapplicability of degenerate impurity models to actinide heavy-fermion compounds.

In conclusion, we have calculated the magnetization as a function of field for the f^1-f^2 Anderson model with $j-j$ coupling for large degeneracies. The overall behaviour shows, for valences away from the f^2 limit, a two-stage crossover as a function of field, due to the partial unbinding of the many-body singlet state. At low fields, the magnetization shows upward curvature only for valences close to the integral values, while for the intermediate valent regime the upward curvature is destroyed. It would be of interest to see to what extent curvature (or its absence) in $M(H)$ can be found in dilute uranium alloys, where the lattice metamagnetic effects should no longer be present.

References

- [1] Hewson A C 1992 *The Kondo Problem to Heavy Fermions* (Cambridge: Cambridge University Press)
- [2] Lee P A, Rice T M, Serene J W, Sham L J and Wilkins J W 1986 *Commun. Solid State Phys.* **12** 99
Brandt N B and Moshchalkov V V 1984 *Adv. Phys.* **33** 373
- [3] Cox D L 1987 *Phys. Rev. Lett.* **59** 1240
- [4] Perakis I E, Varma C M and Ruckenstein A E 1993 *Phys. Rev. Lett.* **70**
- [5] Seaman C, Maple M B, Lee B W, Ghamaty S, Torishvili M S, Kang J S, Liu L Z, Allen J W and Cox D L 1991 *Phys. Rev. Lett.* **67** 2882
- [6] Schlottmann P 1989 *Phys. Rep.* **181** 1

- [7] Yafet Y, Varma C M and Jones B A 1985 *Phys. Rev. B* **32** 360
- [8] Read N, Dhrmvir K, Rasul J W and Newns D M 1986 *J. Phys. C: Solid State Phys.* **19** 1957
- [9] Nunes A C, Rasul J W and Gehring G A 1986 *J. Phys. C: Solid State Phys.* **19** 1017
- [10] Evans S M and Gehring G A 1989 *J. Phys.: Condens. Matter* **1** 3085
- [11] Saso T 1988 *J. Magn. Magn. Mater.* **76-77** 176
Saso T 1992 *Prog. Theor. Phys. Suppl.* **108** 89
- [12] Rasul J W 1990 *Phys. Rev. B* **42** 9996
- [13] Sakai O, Shimizu Y and Kasuya T 1992 *Prog. Theor. Phys. Suppl.* **108** 73
Sakai O, Shimizu Y and Kasuya T 1988 *Physica B* **163** 401
- [14] Landgraf J M and Rasul J W 1992 *Phys. Rev. B* **47** 16 620
- [15] Hewson A C and Rasul J W 1983 *J. Phys. C: Solid State Phys.* **16** 6799
- [16] Hewson A C, Rasul J W and Newns D M 1983 *Solid State Commun.* **47** 59
- [17] Read N and Newns D M 1983 *J. Phys. C: Solid State Phys.* **16** 3273
Read N and Newns D M 1984 *Solid State Commun.* **52** 993
- [18] Withoff D and Fradkin E 1986 *Phys. Rev. B* **34** 8172
- [19] Franse J J M, Frings P H, de Boer F R, Menovsky A, Beers C J, van Deursen A P J, Myron H W and Arko A J 1982 *Phys. Rev. Lett.* **48** 1749
- [20] Ott H R, Rudiger H, Rice T M, Ueda K, Fisk Z, Smith J L 1984 *Phys. Rev. Lett.* **52** 1915
- [21] Yang K N, Torikachvili M S, Maple M B, Ku H C, Pate B B, Lindau I and Allen J W 1985 *J. Magn. Mater.* **47&48** 558
- [22] Buyers W J L 1985 *J. Magn. Mater.* **47&48** 602